Національна академія наук України

ІНСТИТУТ ФІЗИКИ КОНДЕНСОВАНИХ СИСТЕМ

ICMP–16–02E

I.V. Stasyuk, V.O. Krasnov

PHASE TRANSITIONS IN THE HARD-CORE BOSE-FERMI-HUBBARD MODEL AT NON-ZERO TEMPERATURES IN THE HEAVY-FERMION LIMIT

ЛЬВІВ

УДК: 538.945

PACS: 71.10.Fd, 71.38

Фазові переходи у моделі Бозе-Фермі-Хаббарда для жорстких бозонів при ненульових температурах у границі важких ферміонів

І.В. Стасюк, В.О. Краснов

Анотація. Досліджено фазові переходи в суміші надхолодних бозе- та фермі- атомів у оптичній гратці на базі моделі Бозе-Фермі-Хаббарда в наближенні середнього поля та жорстких бозонів. Розглянуто випадок безмежно малого переносу ферміонів; враховано одновузлову бозон-ферміонну взаємодію типу відштовхування. Проаналізовано поведінку параметра порядку бозе-конденсату та термодинамічного потенціалу як функцій хімічних потенціалів частинок при ненульових температурах. Встановлено можливість зміни роду фазового переходу до надплинної фази у режимі фіксованих хімічних потенціалів бозонів та ферміонів. Побудовано відповідні фазові діаграми.

Phase transitions in the hard-core Bose-Fermi-Hubbard model at non-zero temperatures in the heavy-fermion limit

I.V.Stasyuk, V.O. Krasnov

Abstract. The phase transitions in the ultracold Bose- and Fermi-particles mixture in optical lattices using the Bose-Fermi-Hubbard model in the mean field and hard-core boson approximations are investigated. The case of infinitely small fermion transfer and the repulsive on-site boson-fermion interaction is considered. The behavior of the BE condensate order parameter and grand canonical potential as functions of the chemical potentials of particles at non-zero temperatures is analyzed. The possibility of change of order of the phase transition to the superfluid phase in the regime of fixed values of the chemical potentials of Bose- and Fermi-particles is established. The relevant phase diagrams are built.

Препринти Інституту фізики конденсованих систем НАН України розповсюджуються серед наукових та інформаційних установ. Вони також доступні по електронній комп'ютерній мережі на WWW-сервері інституту за адресою http://www.icmp.lviv.ua/

The preprints of the Institute for Condensed Matter Physics of the National Academy of Sciences of Ukraine are distributed to scientific and informational institutions. They also are available by computer network from Institute's WWW server (http://www.icmp.lviv.ua/)

Ігор Васильович Стасюк
Володимир Олександрович Краснов

Фазові переходи у моделі Бозе-Фермі-Хаббарда для жорстких бозонів при ненульових температурах у границі важких ферміонів

Роботу отримано 6 квітня 2016 р.

Затверджено до друку Вченою радою ІФКС НАН України

Рекомендовано до друку відділом квантової статистики

Виготовлено при ІФКС НАН України

1. Introduction

Development of physics of strongly correlated systems of particles is connected during last years to a large extent with investigation of the ultracold Bose- and Fermi-particles behaviour in optical lattices. The main attention is paid to BE-condensation of Bose-atoms (originally observed in 2002-2003 [1, 2] in the system of ^{87}Rb atoms) as well as other collective phenomena and phase transitions connected with this effect. A model, which was named as the Bose-Hubbard model [3, 4] has been proposed for their description. Its analogue and generalization in the case of atomic boson-fermion mixtures is the Bose-Fermi-Hubbard model [5]. Allowance for short-range on-site interparticle interaction of Hubbard type, just as tunneling of particles between the neighbouring minima of potential in the lattice, form a basis of both models.

In the simple cases, the BE condensation of Bose-atoms in optical lattices occurs by the 2nd order phase transition from the Mott insulator phase (MI phase) to the superfluid phase (SF phase). In a lot of investigations based on the Bose-Hubbard (BH) model, the phase diagrams, determining the conditions of the SF phase existence at $T = 0$ and at the non-zero temperatures for the cases of 1d, 2d, and 3d lattices of different symmetry and structure, were built [6–12]; the characteristic features of the single-particle spectrum were investigated (see also reviews [13–15]). Extension of model by inclusion of intersite interactions enabled to describe an appearance of modulated phases, in particular a supersolid (SS) phase [16,17]. On the other hand, it was established that the order of a MI-SF transition can change at some conditions from 2nd to the 1st one in the case when the excited vibrational states (that can be occupied due to optical pumping) of Bose-particles in quantum wells or additional (e.g. spin) degrees of freedom of bosons with $S \geq 1$ are taken into account [18–20]. The effect is caused by competition between the energy gain at the appearance of BE condensate (which is formed by particles in excited states) and the particles excitation energy.

The MI-SF phase transition takes place also in the boson-fermion atomic mixture; it has been observed experimentally, in particular, in the spin-polarized mixture of $^{87}Rb - ^{40}K$ atoms [21–23]. The influence of Fermi-atoms on condensation of bosons is an important problem that remains to be a subject of attention. Interaction with fermions at the increase of their consentration leads to the gradual fading of the coherence of bosons and the decay of condensate fraction in SF phase in a certain range of the values of thermodynamic parameters (chemical potential of bosons or temperature). Such an interaction causes as well the change

of stability regions of SF and MI phases. It manifests, first of all, in the shift of the MI-SF transition lines in the phase diagrams [24, 27]. Due to mentioned interaction, the so-called fermion composites appear, as was shown at $T = 0$ in [28, 29]; they arise as a result of fermion pairing with one or more bosons (or one or more boson holes) because of effective U_{BF} attraction (or repulsion). One can change the value and even the sign of the U_{BF} interaction constant using the Feshbach resonance [30, 31].

Description of equilibrium properties of the mixture of the Bose- and Fermi-atoms in optical lattice, performed on the basis of the Bose-Fermi-Hubbard (BFH) model in [32, 33] using the mean field approximation, had given a possibility to obtain the phase diagrams at $T = 0$ and determine the regions of existence of SF and MI phases, including the phases with fermion composites. In the frames of similar approach, at the exact treatment of boson-fermion interaction, the phase transitions and the BE condensate appearance in the BFH model were investigated at $T \neq 0$ [12]. The consideration was performed in both cases in the regime of fixed fermion concentration and the given values of the boson chemical potential.

Besides the CDW phase with modulation of the particle density or SS phase with modulation of the condensate order parameter (such phases are known for pure boson system in optical lattices),appearance of new quantum phases is a specific feature of the boson-fermion mixtures. To describe them, it is necessary to go out the standard mean field approximation and take into account explicitly the hopping dynamics of bosons and fermions. Here, on the one side, the band transfer of fermions induces an effective interaction $V_{BB}(w, \vec{q})$ between bosons through fermion field [34–36]. Depending on the wave vector $\vec{q}$ value, that corresponds to the possible instability, it can be a reason of phase separation or spatial modulation accompanied by appearance of the mentioned CDW as well as SS phases [37] On the other side, at the spin degeneracy, the reverse effect is possible when pairing of fermions due to transfer of bosons is induced [38–40]. Such an effect is analogous to the electron Cooper pairs creation in the BCS model. The role of superfluid component in the so-called SF_f phase belongs in this case to the fermion pairs; the corresponding phase diagrams were obtained in [41].

Integration over fermionic variables provides also an additional static interaction between bosons, which promotes MI→SF transition or, to the contrary, suppresses it. It depends on relation between masses of Bose- and Fermi atoms (i.e., on the ratio of hopping parameters t_B/t_F). Phase diagrams, obtained within the Gutzwiller approach, illustrate this effect on the examples of "light" (a mixture of $^{87}Rb - ^{40}K$ atoms) and "heavy"

(a mixture of $^{23}Na - ^{40}K$ atoms) fermions [35].

Another aspect of mutual influence of bosons and fermions is connected with "polaron effect", when due to influence of the fermion surroundings the hopping parameter t_B of bosons is reduced and at $T = 0$ the region of SF phase becomes narrower [42]. At the same time, for heavy fermions such a region broadens at the increase of T up to intermediate temperatures [36], and after that the SF phase disappears.

The limiting case of heavy fermions ($t_F \to 0$) was considered separately in our previous work [43]. In this limit, the effective boson-boson and fermion-fermion interactions do not appear, while the direct interspecies interaction can be taken into account exactly. Contrary to the majority of works devoted to the thermodynamics of BFH model, where the consideration has been performed for the $\mu_B = \text{const}$ and $\bar{n}_F = \text{const}$ case, our calculation was made in the regime of given values of chemical potentials of bosons (μ_B) and fermions (μ_F). The change of statistical ensemble and transition to μ_B and μ_F as independent thermodynamic variables enabled to study more detailly the equilibrium states of BFH model basing on the condition of the global minimum of the grand canonical potential Ω. We had used the mean field approximation and restrict ourselves to the case of hard-core bosons, where the occupation of on-site states conforms to the Pauli principle ($n_f = 0, 1$). For Bose-atoms on a lattice this is a limiting case ($U \to \infty$) of the Bose-Hubbard model. The hard-core boson (HCB) model is rather frequently used [44–48]. It is related formally to the region $0 \leq \bar{n}_B \leq 1$, but can also describe the MI-SF transition in the vicinity of points $\mu_B = nU$, where $n = 0, 1, 2, ...$, for finite values of U (when $t_B \ll U$); at that time $n \leq \bar{n}_B \leq n + 1$ [11, 12]. We considered in [43] the spinless fermions having in mind a situation in real systems, when the spin degeneracy is absent (for example, it is removed by applying of external magnetic field). In such a case, the model is a four-state one in the single-site limit.

As was shown in [43], there exist at $T = 0$ the regions of values of the model parameters and chemical potentials, where the order of MI-SF transition changes from the 2nd to the 1st one. It is a consequence of competition between states with $\bar{n}_F = 0$ and $\bar{n}_F = 1$ (at $T = 0$) that manifests itself in such a way in the case, when BE condensate appears. Here the phase separation (into phases with different concentrations of particles) takes place at the given average concentration of bosons.

It is necessary to stress in this connection, that in the most of previous works, including the mentioned above [43] the phase diagrams were built starting from the instability condition of the SF phase. Using this procedure, that defines the spinodal lines, one postulates a priory the

second order of the MI-SF phase transition.

Should be mentioned, that the "'heavy" fermion case was already the subject of attention. As was shown in [26, 32], the frozen fermions are capable to prevent the occurrence of long-range correlations of superfluid type and the appearance of BE condensate. There exists, however, the critical fermion consentration below of which this effect is absent ($\bar{n}_F^{crit} \sim 0,59$ for $d = 2$; $\bar{n}_F^{crit} \sim 0,31$ for $d = 3$; see [26]). In our case, speaking about "heavy" fermion, we have rather in mind the ultimately low values of the hopping parameter t_F.

Our aim in this work is a continuation of investigation, carried out in [43], and extension to the non-zero temperature region. Basing on the hard-core boson approach, we shall consider the changes in the (μ', μ) and ($|t_0|$, μ) phase diagrams, obtained for $T = 0$ (where $\mu = \mu_B$, $\mu' = \mu_F$, $t_0 = t_B(\vec{q} = 0)$). The calculations will be performed, as in [43], for the case of "heavy" fermions considering the boson hopping in the mean field approximation. We shall also build the (T, μ), (μ', μ), and ($|t_0|$, μ) phase diagrams which determine at $T \neq 0$ the regions of the SF phase existence at various values of chemical potential of fermions. The conditions at which the MI-SF transitions are of the 1st order in this case, will be analyzed. We shell also pay an attention to the phase separation problem.

2. Hamiltonian

We start from the Hamiltonian of the Bose-Fermi-Hubbard model written in the form

$$H = \frac{U}{2}\sum_i n_i^b(n_i^b - 1) + U'\sum_i n_i^b n_i^f - \mu\sum_i n_i^b - \mu'\sum_i n_i^f + \\ + \sum_{<i,j>} t_{ij} b_i^+ b_j + \sum_{<i,j>} t'_{ij} a_i^+ a_j \qquad (2.1)$$

Here U and U' are constants of boson-boson and boson-fermion on-site interactions; μ and μ' are chemical potentials of bosons and fermions, respectively (we consider here the case of repulsive interactions $U > 0, U' > 0$) and $t(t')$ are tunneling amplitudes of bosons (fermions) describing the boson (fermion) hopping between nearest lattice sites.

Let us introduce the Hubbard operators $X_i^{n,m} = |n,i\rangle\langle m,i|$ and $X_i^{\tilde{n},\tilde{m}} = |\tilde{n},i\rangle\langle\tilde{m},i|$ acting on the single-site basis of states

$$(n_i^b = n; n_i^f = 0) \equiv |n,i\rangle; \quad (n_i^b = n; n_i^f = 1) \equiv |\widetilde{n},i\rangle \qquad (2.2)$$

where $n_i^b(n_i^f)$ are occupation numbers of bosons (fermions) on the site i. In the hard-core boson limit ($U \to \infty$) the basis consists of four states

$$|0\rangle = |0,0\rangle, \qquad |\widetilde{0}\rangle = |0,1\rangle \\ |1\rangle = |1,0\rangle, \qquad |\widetilde{1}\rangle = |1,1\rangle \qquad (2.3)$$

In this case, when the restriction $n = 0, 1$ and $\tilde{n} = \tilde{0}, \tilde{1}$ on occupation numbers is imposed,

$$b_i = \sum_n \sqrt{n+1} X_i^{n,n+1} + \sum_{\widetilde{n}} \sqrt{\widetilde{n}+1} X_i^{\widetilde{n},\widetilde{n}+1} \to X_i^{01} + X_i^{\tilde{0}\tilde{1}} \\ a_i = \sum_n X_i^{n,\widetilde{n}} \to X_i^{0\tilde{0}} + X_i^{\tilde{1}\tilde{1}} \\ n_i^b = \sum_n n X_i^{n,n} + \sum_{\widetilde{n}} \widetilde{n} X_i^{\widetilde{n},\widetilde{n}} \to X_i^{11} + X_i^{\tilde{1}\tilde{1}} \\ n_i = \sum_{\widetilde{n}} X_i^{\widetilde{n},\widetilde{n}} \to X_i^{\tilde{0}\tilde{0}} + X_i^{\tilde{1}\tilde{1}} \qquad (2.4)$$

The Hamiltonian (2.1) in this new representation can be written as

$$\hat{H} = \sum_i \left(\lambda_0 X_i^{00} + \lambda_1 X_i^{11} + \lambda_{\tilde{0}} X_i^{\tilde{0}\tilde{0}} + \lambda_{\tilde{1}} X_i^{\tilde{1}\tilde{1}}\right) + \sum_{\langle ij\rangle} t_{ij} b_i^+ b_j, \qquad (2.5)$$

where

$$\lambda_0 = 0; \lambda_1 = -\mu; \lambda_{\tilde{0}} = -\mu'; \lambda_{\tilde{1}} = -\mu - \mu' + U' \qquad (2.6)$$

In the following , we shall consider the case of the so-called heavy fermions, when the inequalities $t' \ll t$ and $t' \ll U'$ are fulfilled, and the fermion hopping between lattice sited can be neglected. On this assumption we had put in (2.5) $t'_{ij} \to 0$.

3. Mean field approximation (MFA)

To describe the transition into SF phase and appearance of BE condensate, we introduce the order parameter $\varphi = \langle b_i\rangle = \langle b_i^+\rangle$. In the case of mean field approach a standard approximation

$$b_i^+ b_j \to \varphi(b_i^+ + b_i) - \varphi^2 \\ \sum_{ij} t_{ij} b_i^+ b_j = \varphi t_0 \sum_i (b_i^+ + b_i) - N t_0 \varphi^2 \qquad (3.1)$$

is used (here $t_0 = \sum t_{ij} = -|t_0|, t_0 < 0$)

Then, after separating the mean-field part of the Hamiltonian (2.5) we shall have

$$H_{MF} = \sum_i H_i - N t_0 \varphi^2; \quad H_i = \sum_{pr} H_{pr} X_i^{pr}; \tag{3.2}$$

and

$$||H_{pr}|| = \left(\begin{array}{cccc|c} |0\rangle & |1\rangle & |\widetilde{0}\rangle & |\widetilde{1}\rangle & \\ \hline 0 & t_0\varphi & 0 & 0 & |0\rangle \\ t_0\varphi & -\mu & 0 & 0 & |1\rangle \\ 0 & 0 & -\mu' & t_0\varphi & |\widetilde{0}\rangle \\ 0 & 0 & t_0\varphi & -\mu-\mu'+U' & |\widetilde{1}\rangle \end{array}\right) \tag{3.3}$$

In is easy to diagonalize the matrix H_{pr} written in the 4-state basis. As a result, we get

$$H_i = \sum_{p'} \varepsilon_{p'} X_i^{p'p'} \tag{3.4}$$

where $p' = 0', 1', \widetilde{0}'$, and $\widetilde{1}'$ are indices which denote the state of new basis and

$$\begin{aligned} \varepsilon_{0',1'} &= -\frac{\mu}{2} \pm \sqrt{\frac{\mu^2}{4} + t_0^2\varphi^2}, \\ \varepsilon_{\widetilde{0}',\widetilde{1}'} &= -\mu' - \frac{\mu}{2} + \frac{U'}{2} \pm \sqrt{\frac{(U'-\mu)^2}{4} + t_0^2\varphi^2} \end{aligned} \tag{3.5}$$

The partition function in MFA is equal to

$$Z_{MF} = Sp\mathrm{e}^{-\beta H_{MF}} = \mathrm{e}^{\beta N t_0 \varphi^2} Z_0^N, \tag{3.6}$$

where

$$Z_0 = e^{-\beta\varepsilon_{0'}} + e^{-\beta\varepsilon_{1'}} + e^{-\beta\varepsilon_{\widetilde{0}'}} + e^{-\beta\varepsilon_{\widetilde{1}'}} \tag{3.7}$$

Accordingly, the grand canonical potential is

$$\Omega_{MF}/N = |t_0|\varphi^2 - \theta \ln Z_0 \tag{3.8}$$

4. Phase diagrams

In our study, we consider the case of fixed chemical potentials of bosons μ and fermions μ'. The thermodynamic equilibrium conditions are determined by grand canonical potential Ω as function of μ, μ' and T. Equilibrium values of the order parameter φ should by found from the global minimum condition of Ω.

In the mean field approximation we have an equation

$$\frac{\partial(\Omega_{MF}/N)}{\partial\varphi} = 2|t_0|\varphi - \frac{\theta}{Z_0}\frac{\partial Z_0}{\partial\varphi} = 0 \tag{4.1}$$

or

$$2|t_0|\varphi + \sum_{p'} \langle X^{p'p'}\rangle \frac{\partial\varepsilon_{p'}}{\partial\varphi} = 0 \tag{4.2}$$

Here the averages $\langle X^{p'p'}\rangle$ are expressed in terms of Boltzmann's factors: $\langle X^{p'p'}\rangle = Z_0^{-1}\exp(-\beta\varepsilon_{p'})$.

The equation (4.2) has the trivial $\varphi = 0$ and nontrivial $\varphi \neq 0$ solutions. For the second one the equation

$$\frac{1}{|t_0|} = \frac{\langle X^{1'1'}\rangle - \langle X^{0'0'}\rangle}{2\sqrt{\frac{\mu^2}{4} + t_0^2\varphi^2}} + \frac{\langle X^{\widetilde{1}'\widetilde{1}'}\rangle - \langle X^{\widetilde{0}'\widetilde{0}'}\rangle}{2\sqrt{\frac{(U'-\mu)^2}{4} + t_0^2\varphi^2}} \tag{4.3}$$

is obtained. In the case of several solutions of this equation, one should separate out those, which are related to minimum values of Ω_{MF}.

If we substitute $\varphi = 0$ in the equation (4.3), we shall obtain the condition of the second order phase transition to the SF phase (if such a transition is possible). In general, it is a condition of instability of normal (MI) phase with respect to the BE condensate appearance (in phase diagrams it corresponds to the spinodal lines).

At $\varphi = 0$ the equation (4.3) takes the form

$$\frac{1}{|t_0|} = \frac{\langle X^{11}\rangle - \langle X^{00}\rangle}{\mu} + \frac{\langle X^{\widetilde{0}\widetilde{0}}\rangle - \langle X^{\widetilde{1}\widetilde{1}}\rangle}{U'-\mu} \tag{4.4}$$

This equation is the same as obtained for the four-state model in [49] from the condition of divergence of the boson Green's function (calculated in the random phase approximation) at $\omega = 0, \vec{q} = 0$. This fact confirms that the relation (4.4) is the condition of instability of the phase with $\varphi = 0$, being therefore an equation for spinodal line (the curve, that determines the borders of the normal phase stability region).

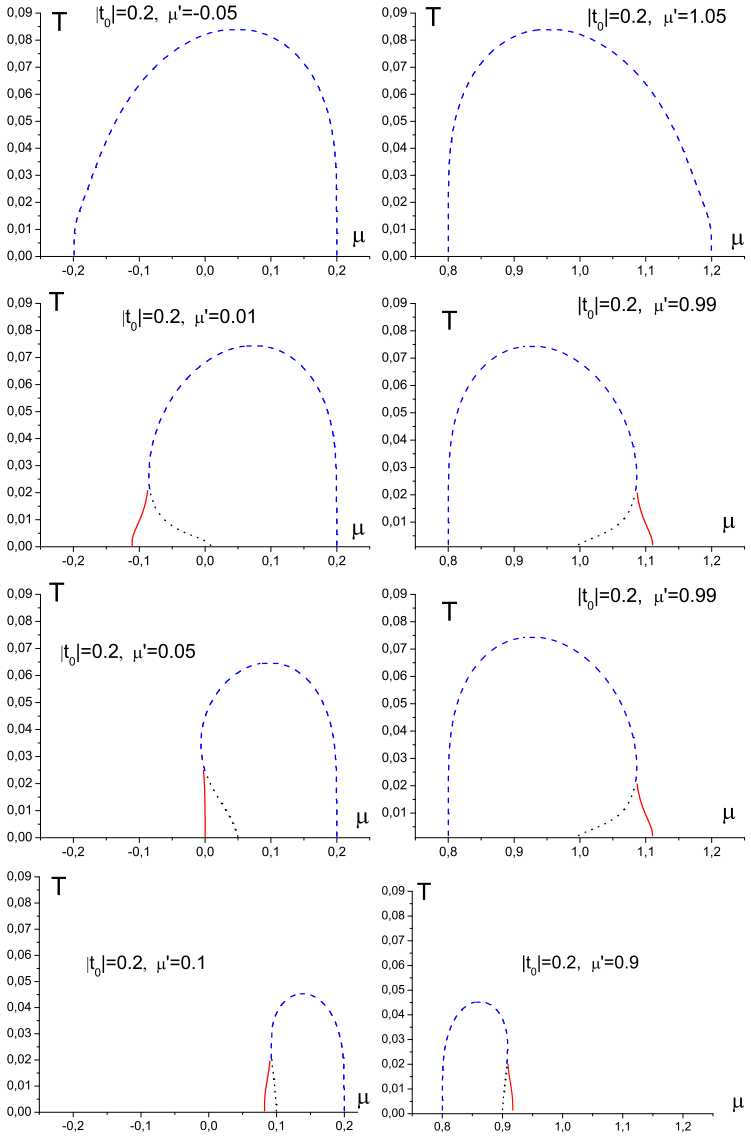

Figure 1. (T, μ) phase diagrams for different values of μ'; $|t_0| = 0.2, U' = 1.0$. Here and henceforth the solid (dashed) lines are the lines of the 1st (2nd) order PT; the dotted and dashed lines correspond to spinodales. All quantities having a dimension of energy are given in U' units. To shorten the notations we use in diagrams an abbreviation T for $\Theta = kT$.

Solutions of the equation (4.4) on the plane (T, μ) for different values of μ' are shown in figures 1, 2, and 3 .

Outside the $[0, U']$ interval for μ', the curves of spinodals have the usual dome-like shape which gradually takes the symmetric form at the $|\mu'|$ increase.

Attaining to this area, the curves undergo an appreciable deformation, and when they enter inside, the regions with two temperatures of instability corresponding to one value of μ appear. With the change of T the "re-entrant" transitions became possible. Hence, to get the real (T, μ) phase diagrams (figs. 1- 4) one need to investigate the grand canonical potential behaviour in such regions.

Analysis, performed for the case $T = 0$ in [43], shows that in these regions (especially when $\mu' \gtrsim 0$ and $\mu' \lesssim U'$) the order of MI-SF transition can change from 2nd to the 1st one. From figures 5 and 6 one can see how the shapes of curves for $\varphi(\mu)$ and $\Omega_{MF}/N(\mu)$ change with the increase of temperature in the region of parameters values, where at $T = 0$ we have the first order phase transition. Here are two variants (see [43]).

The first one (i) realizes at the μ' values $0 < \mu' < |t_0|$ or $U' - |t_0| < \mu' < |t_0|$ in the case $|t_0| < U'/2$ and at the μ' values $0 < \mu' < U'^2/4|t_0|$ or $U' - U'^2/4|t_0| < \mu' < U'/2$ in the case $U' > |t_0| > \frac{U'}{2}$. The second one (ii) takes place only in the case $U' > |t_0| > U'/2$, when $U'^2/4|t_0| < \mu' < U' - U'^2/4|t_0|$.

In the first of them (variant (i)) the 2nd order phase transition is replaced in the low temperature region by the 1-st order one. The line of the latter passes on the (T, μ) plane (figure 2) to the left (right) of the spinodal line at $\mu' < U'/2$ ($\mu' > U'/2$). It is seen from behaviour of $\varphi(\mu)$ and $\Omega_{MF}/N(\mu)$ curves in the mentioned intervals of chemical potentials values (figure 5). At higher temperatures the reverse course of $\varphi(\mu)$ function and "fishtail" of Ω_{MF}/N gradually decreases and disappeares. At certain temperature we reach the tricritical point, and the order of phase transition changes to the second one. At the further increase of temperature the curve of phase transition coincides with the spinodal line. It is shown in figures 1 and 2, where solid lines are the lines of the first order phase transitions.

The variant (ii) differs form the first one in position of the first order phase transition line that is placed here inside the region of SF phase. At $T = 0$, it separates this region on two parts which are characterized by different mean occupation of fermion states. Sequence of graphs in figure 6. illustrates a gradual disappearing of reverse course of $\varphi(\mu)$ (as well as corresponding feature of $\Omega(\mu)$) at the temperature increase. The

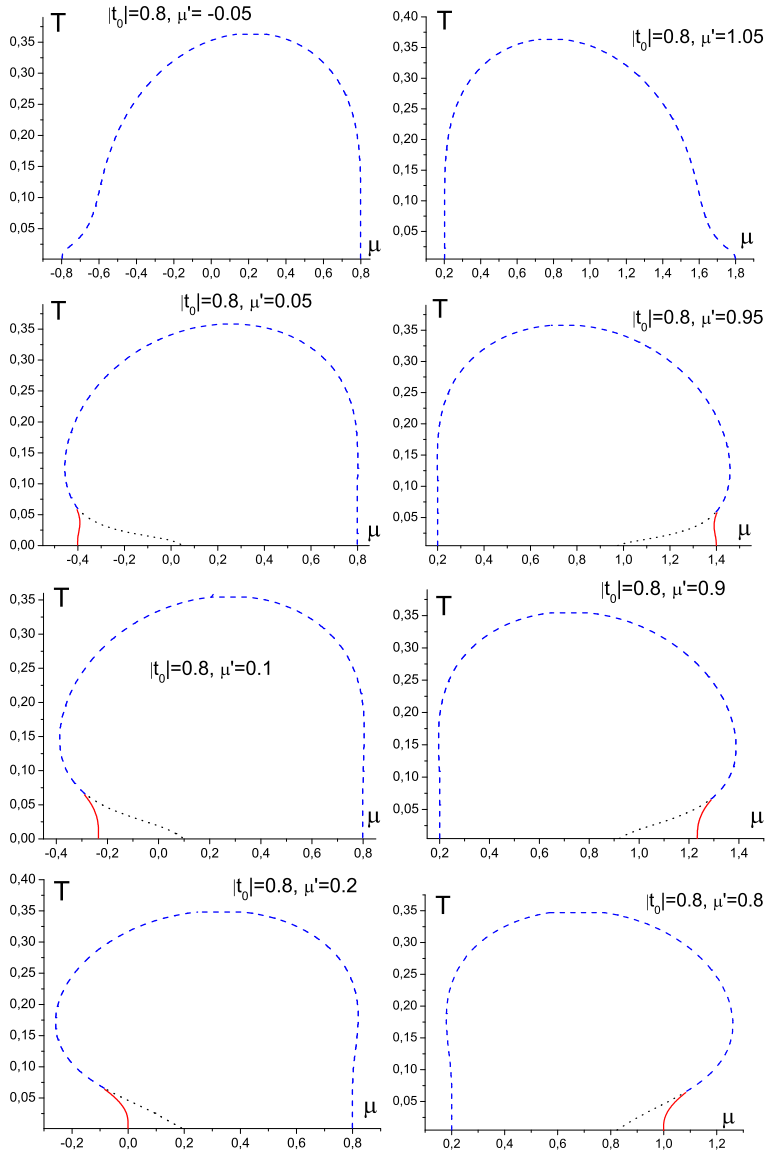

Figure 2. (T, μ) phase diagram for different values of μ'; $|t_0| = 0.8, U' = 1.0$. The cases $0 < \mu' < U'^2/4|t_0|$ and $U' - U'^2/4|t_0| < \mu' < U'/2$. Here $U'/2 < |t_0| < U'$.

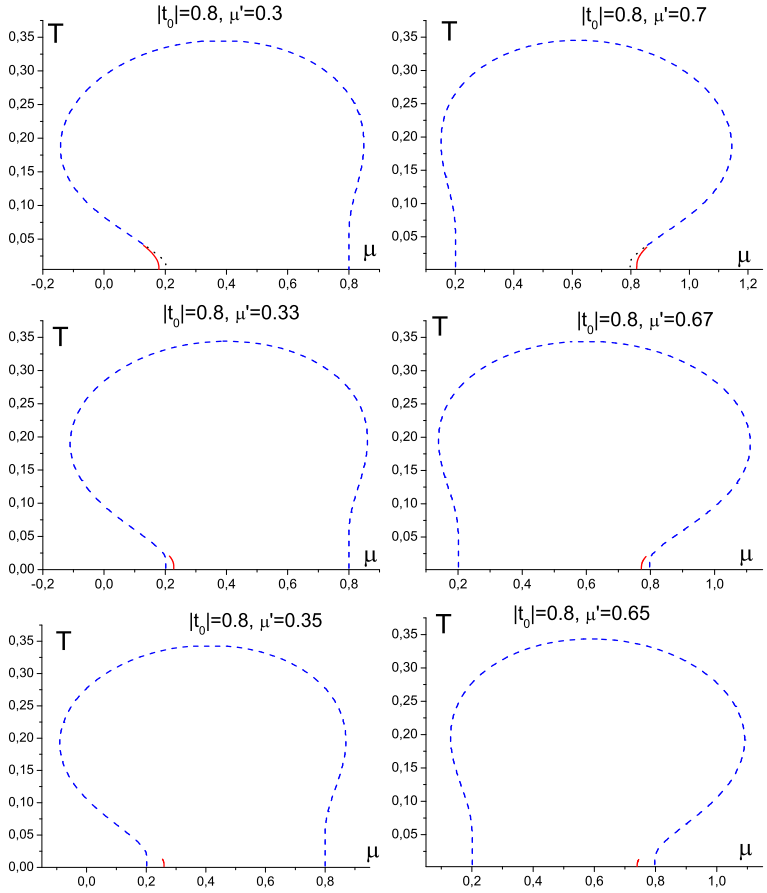

Figure 3. (T, μ) phase diagram for different values of μ'; $|t_0| = 0.8, U' = 1.0$. The case $U'^2/4|t_0| < \mu' < U' - U'^2/4|t_0|$ at $U'/2 < |t_0| < U'$.

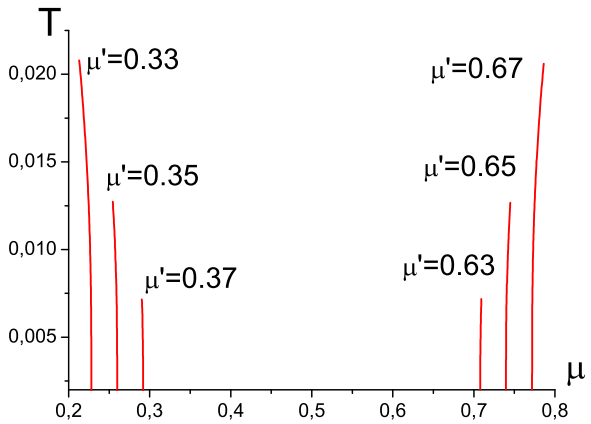

Figure 4. First order phase transition lines on the (T, μ) plane for different values of μ'; $|t_0| = 0.8, U' = 1.0$. The case $U'^2/4|t_0| < \mu' < U' - U'^2/4|t_0|$ at $U'/2 < |t_0| < U'$.

transition line terminates in a critical point that is located within the SF phase area (figure 3). The transitions from this phase into the normal (MI) one are of the 2-nd order. Temperatures of critical points become lower when μ' shifts to the centre of $[0, U']$ interval (see figure 4); in this limit the 1st order phase transition at $T \neq 0$ disappears.

One can see from figures 2 and 3 that in almost all cases for $0 < \mu' < U'$ interval there are regions where "re-entrant" transitions take place. In these cases the SF phase exists as intermediate one between temperature regions where the normal phase is stable.

Let us consider now, besides previously analyzed, the phase diagrams (μ', μ) at nonzero temperatures. We begin with the case of low temperatures when the regions of μ' (and μ) values with phase transitions of the 1-st order are present. The (μ', μ) diagrams possess here a different form for $|t_0| < U'/2$ and $U'/2 < |t_0| < U'$. The transformation of such diagrams, obtained numerically, at the increase of T is shown in figures 7 and 8. As can be seen, a gradual shortening of the 1st order PT lines in the first case, as well as a breaking of such a line at $T \neq 0$ in the region $U' - |t_0| < \mu < |t_0|$ and subsequent reduction of the mentioned PT regions at higher T in the second case, take place.

In the region of temperatures above the critical and tricritical ones the phase transition lines coincide with spinodales; the transitions, as such, are of the 2nd order. Borders between phases are determined in

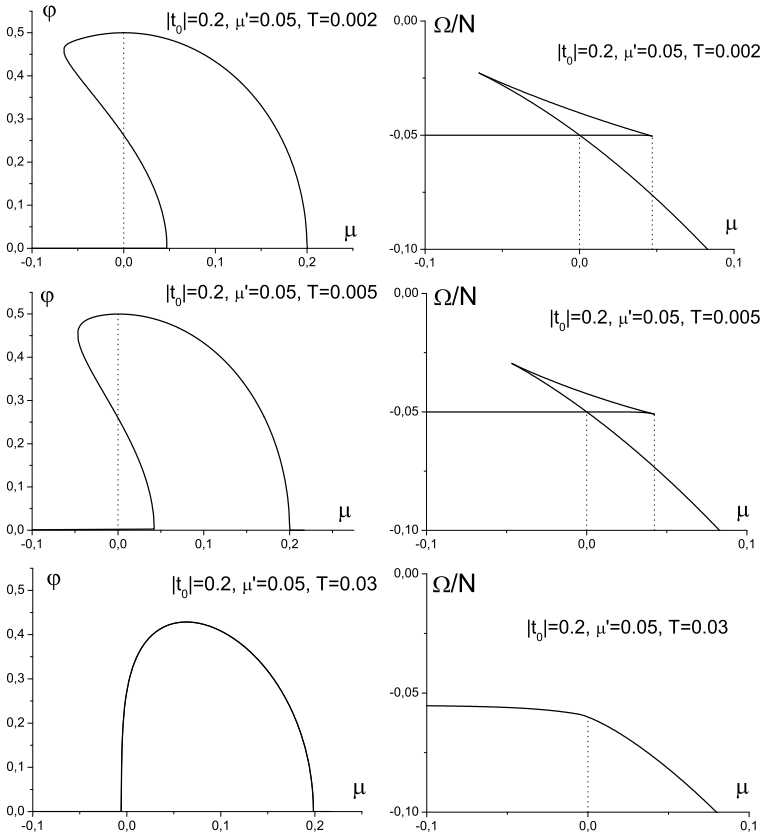

Figure 5. The $\varphi(\mu)$ and $\Omega_{MF}/N(\mu)$ dependences for different values of T at $|t_0| = 0.2, \mu' = 0.05$.

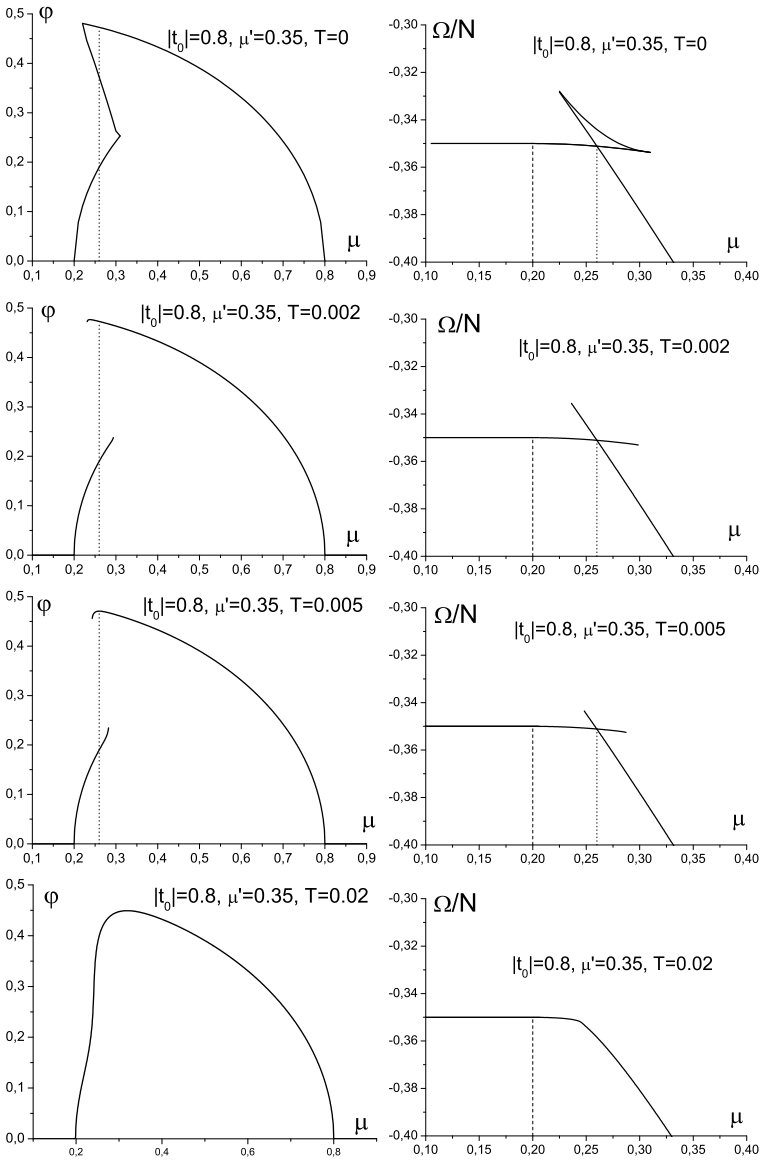

Figure 6. The $\varphi(\mu)$ and $\Omega_{MF}/N(\mu)$ dependences for different values of T at $|t_0| = 0.8, \mu' = 0.35$.

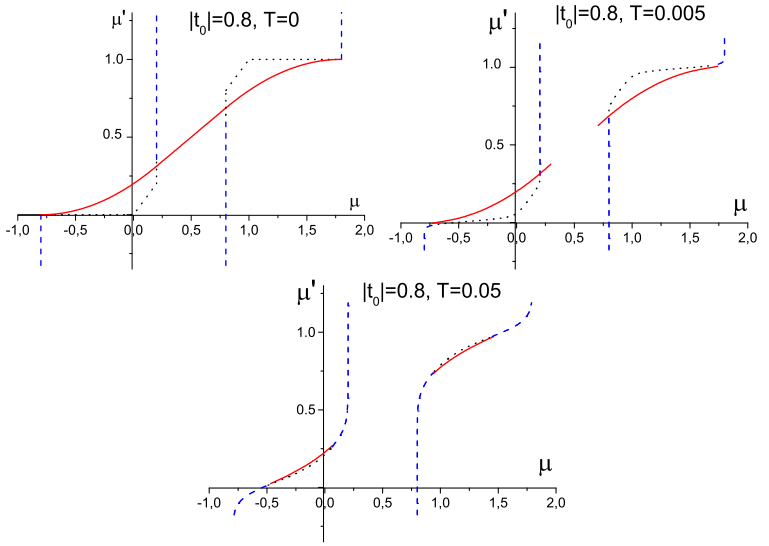

Figure 7. Phase diagrams (μ', μ) for $|t_0| = 0.8, U' = 1.0$. The case $U'/2 < |t_0| < U'$.

this case by the equation (5.4) where

$$\langle X^{nn}\rangle = Z_0^{-1}\,|_{\varphi=0}\, e^{-\beta\lambda_n}; \quad \langle X^{\tilde{n}\tilde{n}}\rangle = Z_0^{-1}\,|_{\varphi=0}\, e^{-\beta\lambda_{\tilde{n}}}$$
$$Z_0\,|_{\varphi=0} = \sum_{n=0}^{1} e^{-\beta\lambda_n} + \sum_{n=\widetilde{0}}^{\widetilde{1}} e^{-\beta\lambda_{\tilde{n}}} \tag{4.5}$$

and λ_n and $\lambda_{\tilde{n}}$ are specified in (1.5).

In the case $U'/2 < |t_0| < U'$, the obtained numerically at low temperatures (μ', μ) phase diagrams are presented in figure 7. The change of shape of the SF phase region during gradual raising of temperature, starting from $\Theta = 0,1U'$, is shown in figure 9. This region is simply connected at $T = 0$. However, as is seen from μ' versus μ plots, at certain (critical) temperature Θ_c the change of topology of phase diagrams takes place. The SF phase region becomes biconnected (it occurs at $\Theta_c \cong 0,341U'$ when $|t_0| = 0,8U'$). Such a splitting into two parts is realized at point with coordinates $\mu = \mu' = 0,5U'$. For these values of chemical potentials we have at Θ_c the second order phase transition from the SF to MI phase.

At the further increase of temperature the separated regions of SF

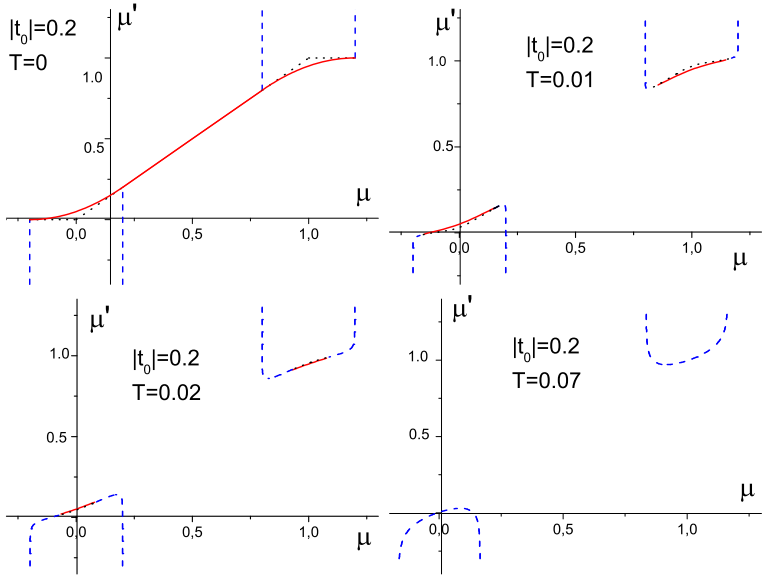

Figure 8. Phase diagrams (μ', μ) for $|t_0| = 0.2$. The case $0 < |t_0| < U'/2$.

phase move away one from another and become narrower. Finally, they disappear at $\Theta_c^0 = |t_0|/2$. This temperature is obtained from the equations

$$\frac{1}{|t_0|} = \frac{1}{\mu} \tanh \frac{\beta\mu}{2} \tag{4.6}$$

or

$$\frac{1}{|t_0|} = \frac{1}{\mu - U'} \tanh \frac{\beta(\mu - U')}{2} \tag{4.7}$$

at large negative or positive values of μ'. The temperature Θ_c^0 has a meaning of maximum temperature at which the SF phase in the pure hard-core boson case disappears (in the mean-field approximation). When $\mu' < 0, \quad |\mu'| \gg U'$, the fermions are practically absent ($\overline{n}_f \approx 0$), while at $\mu' > 0, \quad |\mu'| \gg U'$ the almost all lattice sites are occupied by fermions ($\overline{n}_f \approx 1$). In both limits the fermions have no influence on phase transition in boson subsystem shifting only the critical value of the boson chemical potential. Phase transitions curves in the (T, μ) plane have a form of domes, which are symmetrical with respect to $\mu = 0$ or $\mu = U'$ points (where the maxima of domes are located).

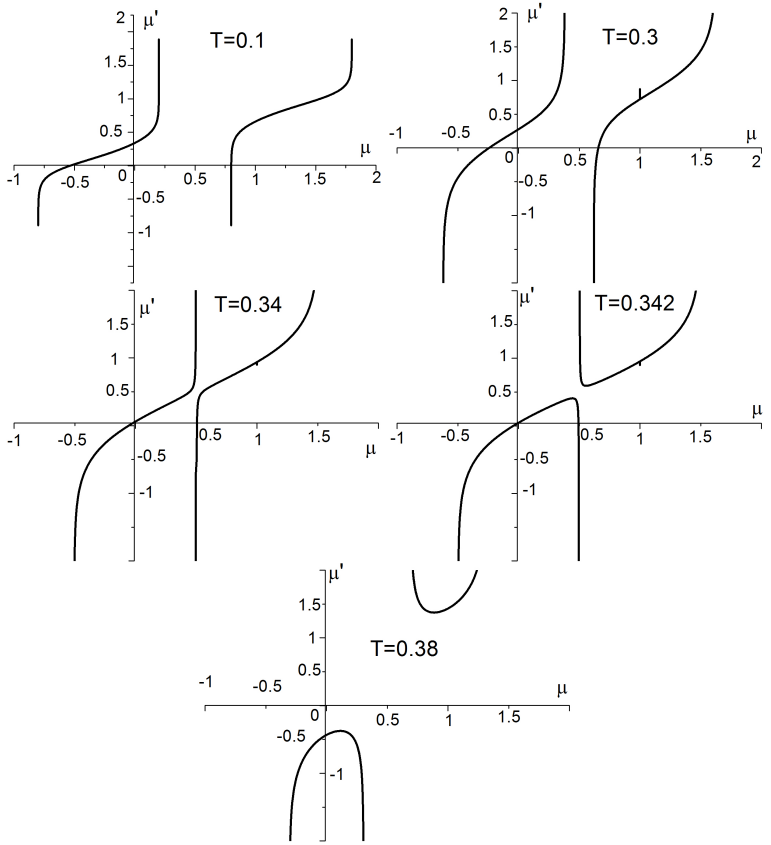

Figure 9. The change of shape of the SF phase region on the (μ', μ) plane during gradual raising of temperature; $|t_0| = 0.8$. The case $U'/2 < |t_0| < U'$.

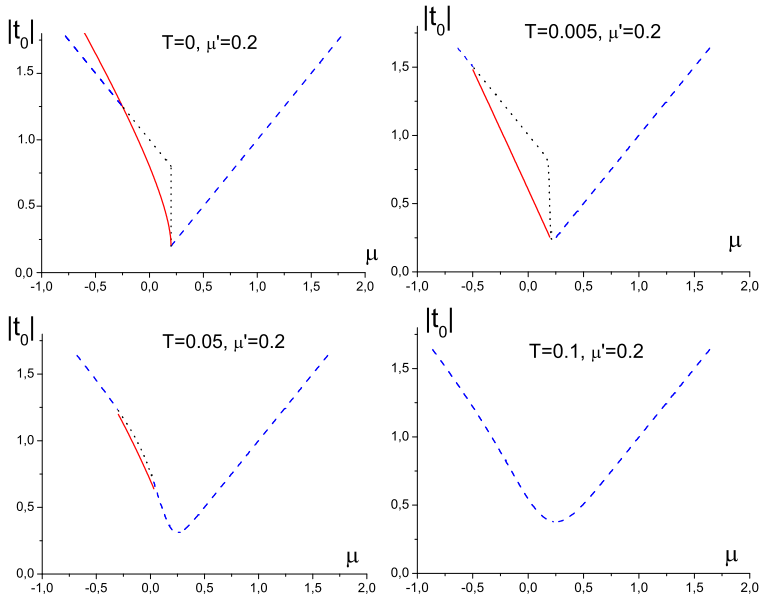

Figure 10. $(|t_0|, \mu)$ phase diagrams for $\mu' = 0.2, U' = 1.0$. The case $0 < \mu' < U'/2$.

An additional information about the phase transition picture in the model can be obtained from the $(|t_0|, \mu)$ diagrams. Such diagrams at given T were built using the set of (T, μ) and (μ', μ) phase diagrams; some examples are presented in figures 10 and 11.

The sequence of graphs in figure 10 illustrates the changes in conditions of existence of SF and MI phases as well as gradual disappearing of the 1st order PT line at the temperature increase (what is in accordance with previous data). Comparing with diagrams related to the $|t_0| < U'/2$ case, we present in figure 11 the diagrams for $U'/2 < |t_0| < U'$. There exists a one-to-one correspondence between them at the replacement $\mu' \to U' - \mu'$ and the mirror reflection $\mu \to U - \mu$. Phase transitions of the 1st order take place here between SF phase and: i) normal (MI) phase with low concentration of fermions (below half-filling) at $\mu > U'/2$; ii) normal (MI) phase with high concentration of fermions (above half-filling) at $\mu < U'/2$.

The case $\mu' = U'/2$ is here a special one. The corresponding $(|t_0|, \mu)$ phase diagrams at different temperatures are shown in figure 12. For this value of μ', the PT at $T \neq 0$ is of the second order. SF region shifts to

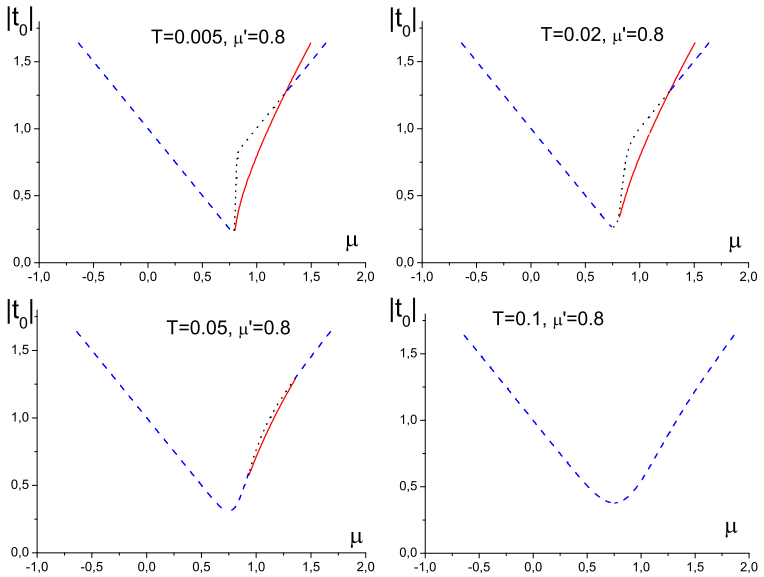

Figure 11. $(|t_0|, \mu)$ phase diagrams for $\mu' = 0.8, U' = 1.0$. The case $U'/2 < \mu' < U'$.

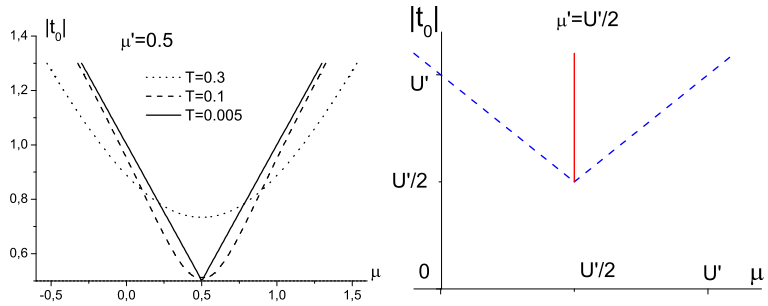

Figure 12. $(|t_0|, \mu)$ phase diagrams at the non-zero temperatures (left) and for $T = 0$ (right). The case $\mu' = U'/2$

higher values of $|t_0|$ at the increase of T, becomes wider (along a μ axis direction) at the beginning, but narrows after that and disappears at high enough temperatures. Such a behaviour is in agreement with (T, μ) diagram at $\mu = U'/2$ (see figure 13).

The symmetric case when $\mu = U'/2$ (corresponding to the half-filling of bosons ($\overline{n}_B = 1/2$)) is worth of separate investigation. Consideration of thermodynamics of the model greatly simplifies here.

The energies of local states (3.5) in such a case are:

$$\varepsilon_{0',1'} = -\frac{U'}{4} \pm \sqrt{\left(\frac{U'}{4}\right)^2 + t_0^2\varphi^2},$$
$$\varepsilon_{\widetilde{0}',\widetilde{1}'} = -\mu' + \frac{U'}{4} \pm \sqrt{\left(\frac{U'}{4}\right)^2 + t_0^2\varphi^2} \qquad (4.8)$$

Respectively, for partition function we have:

$$Z_0 = 2\left(e^{\frac{\beta U'}{4}} + e^{\beta\mu'}e^{\frac{-\beta U'}{4}}\right)\cosh\left(\beta\sqrt{(U'/4)^2 + t_0^2\varphi^2}\right), \qquad (4.9)$$

and for equation for order parameter

$$\frac{1}{|t_0|} = \frac{\langle X^{1'1'}\rangle - \langle X^{0'0'}\rangle + \langle X^{\widetilde{1}'\widetilde{1}'}\rangle - \langle X^{\widetilde{0}'\widetilde{0}'}\rangle}{2\sqrt{(U'/4)^2 + t_0^2\varphi^2}} = \qquad (4.10)$$
$$\frac{\sinh\left(\beta\sqrt{(U'/4)^2 + t_0^2\varphi^2}\right)}{\sqrt{(U'/4)^2 + t_0^2\varphi^2}} \frac{\left(e^{\frac{\beta U'}{4}} + e^{\beta\mu'}e^{\frac{-\beta U'}{4}}\right)}{Z_0}$$

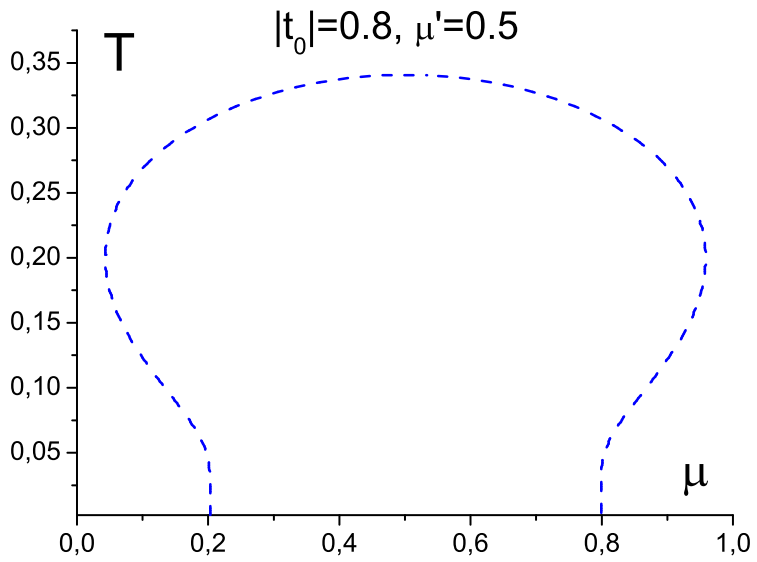

Figure 13. (T, μ) phase diagram in the case $\mu' = U'/2$

After substitution the expression (4.9) we obtain the following equation

$$\sqrt{(U'/4)^2 + t_0^2\varphi^2} = \frac{|t_0|}{2}\tanh\left(\beta\sqrt{(U'/4)^2 + t_0^2\varphi^2}\right) \qquad (4.11)$$

using this equation, the non-zero solution for φ can be found.

As a result, we can consider the behaviour of radical $\sqrt{(U'/4)^2 + t_0^2\varphi^2} \equiv Q$ as function of temperature. The quantity Q is a descending function of temperature $\Theta = 1/\beta$, but it does not reach the zero with the temperature increase and terminates at the $Q_{min} = U'/4$ value, which corresponds to the point, at which the φ parameter goes to zero. Starting from this we can make two conclusions:

1. Non-zero solutions for φ exist only when $Q_{min} < \frac{|t_0|}{2}$, i.e. when $|t_0| > U'/2$.

2. The value $Q = Q_{min}$ corresponds to the spinodal temperature which is determined by the equation

$$U'/4 = \frac{|t_0|}{2}\tanh\beta U'/4 \qquad (4.12)$$

(it follows from (4.11) when $\varphi = 0$). This leads to expression

$$\Theta_{spinod.} = \frac{U'/4}{Arth\frac{U'}{2|t_0|}} \tag{4.13}$$

From equation (4.11) one can see that order parameter φ is a gradually decreasing function of temperature, which tends to zero when $\Theta \to \Theta_{spinod.}$

It is important to stress, that the order parameter φ and temperature Θ_c do not depend on chemical potential of fermions μ'. It holds true for whole region of the μ' values (not only for the $0 < \mu' < U'$ interval, but also for $\mu' < 0$ and $\mu' > U'$). In considered case, the fermion subsystem has an effect on temperature of transition to the state with BEC only through interaction U' with bosons. Here, the critical value $U'_{crit} = 2|t_0|$ exists. When U' exceeds such a value, SF phase in symmetrical case $\mu = U'/2$ disappears (see figure 14).

The foregoing shows that at the temperature $\Theta_{spinod.}$ is the same as that one, at which the SF phase region splits into two separate parts (such an effect was discussed above). The phase transition to SF phase in this case, is of the second order.

Starting from the expression (4.4) for grand canonical potential, we can calculate by means of differentiation the mean boson and fermion

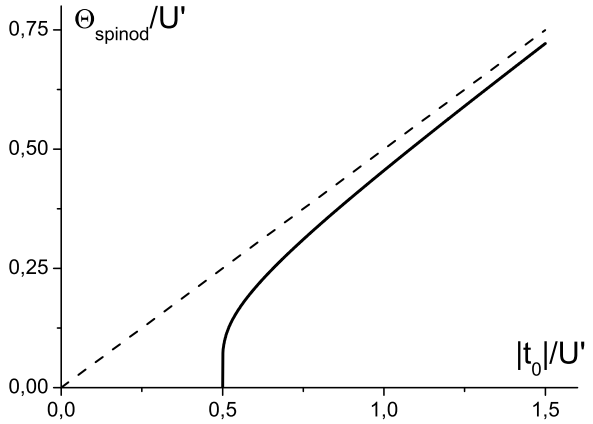

Figure 14. The temperature $\Theta_{spinod.}$ as function of $|t_0|$. Dotted line corresponds to the temperature $\Theta_c^0 = kT_c^0$.

concentrations

$$\bar{n}_B = -\frac{1}{N}\frac{\partial \Omega_{MF}}{\partial \mu}; \quad \bar{n}_F = -\frac{1}{N}\frac{\partial \Omega_{MF}}{\partial \mu'}; \tag{4.14}$$

As a result, using (3.8) and (4.2), we obtain

$$\begin{aligned} \bar{n}_B = \frac{1}{2} &- \frac{\mu}{4\sqrt{\mu^2/4 + t_0^2\varphi^2}} \left\langle X^{0'0'} - X^{1'1'} \right\rangle \\ &- \frac{\mu - U'}{4\sqrt{\frac{(U'-\mu)^2}{4} + t_0^2\varphi^2}} \left\langle X^{\tilde{0}'\tilde{0}'} - X^{\tilde{1}'\tilde{1}'} \right\rangle \\ \bar{n}_F &= \left\langle X^{\tilde{0}'\tilde{0}'} + X^{\tilde{1}'\tilde{1}'} \right\rangle \end{aligned} \tag{4.15}$$

The order parameter φ should be excluded from these expressions by substitution its equilibrium value ($\varphi = 0$, for MI phase and the solution of equation (4.10), for SF phase). Finally, we shall get the averages $\bar{n}_B$ and $\bar{n}_F$ as functions of chemical potentials μ and μ' as well as the temperature.

The concentrations change jump-like on the lines of the 1-st order PT. Their values on these lines are presented in figures 15 and 16 in the form of $\bar{n}_B(\mu')$ and $\bar{n}_F(\mu')$ plots. For each given μ' the limiting values $\bar{n}_B^+$ and $\bar{n}_B^-$ ($\bar{n}_F^+$ and $\bar{n}_F^-$), obtained at the tending to the PT line from the one and another side (that is, from the MI and SF phases), are drawn.

The values of the jumps $\Delta\bar{n}_B = \bar{n}_B^+ - \bar{n}_B^-$ and $\Delta\bar{n}_F = \bar{n}_F^+ - \bar{n}_F^-$ change with temperature decreasing in size at the rising of T. There exist two separate intervals of μ' with a such jump-like behaviour of concentrations; they join together and form the one ($0 < \mu' < U'$) in the limit $T \to 0$ in the case $U'/2 < |t_0| < U'$ (fig. 15). At high temperatures the jumps $\Delta\bar{n}_{B,F}$ disappear (along with the PT order change from the 1st to the 2nd one).

Existence of jumps of Bose- and Fermi-particles concentrations (when crossing the PT line between MI and SF phases) can be considered as a manifestation of possibility of the phase separation in the system, when the concentrations are fixed at the intermediate values. At that time, the separation would consist in segregation into regions with MI and SF phases. At low temperatures, when $|t_0| < U'/2$ and $\mu' \gtrsim 0$, the MI phase is filled mainly by fermions, while in the SF phase the BE condensate is characterized by intermediate concentration of bosons, and concentration of fermions is low. In the $u'/2 < |t_0| < U'$ and $\mu' \lesssim U'$ case, the intrinsic character of phases is another: in MI phase the boson concentration dominates, while in SF phase the BE condensate with

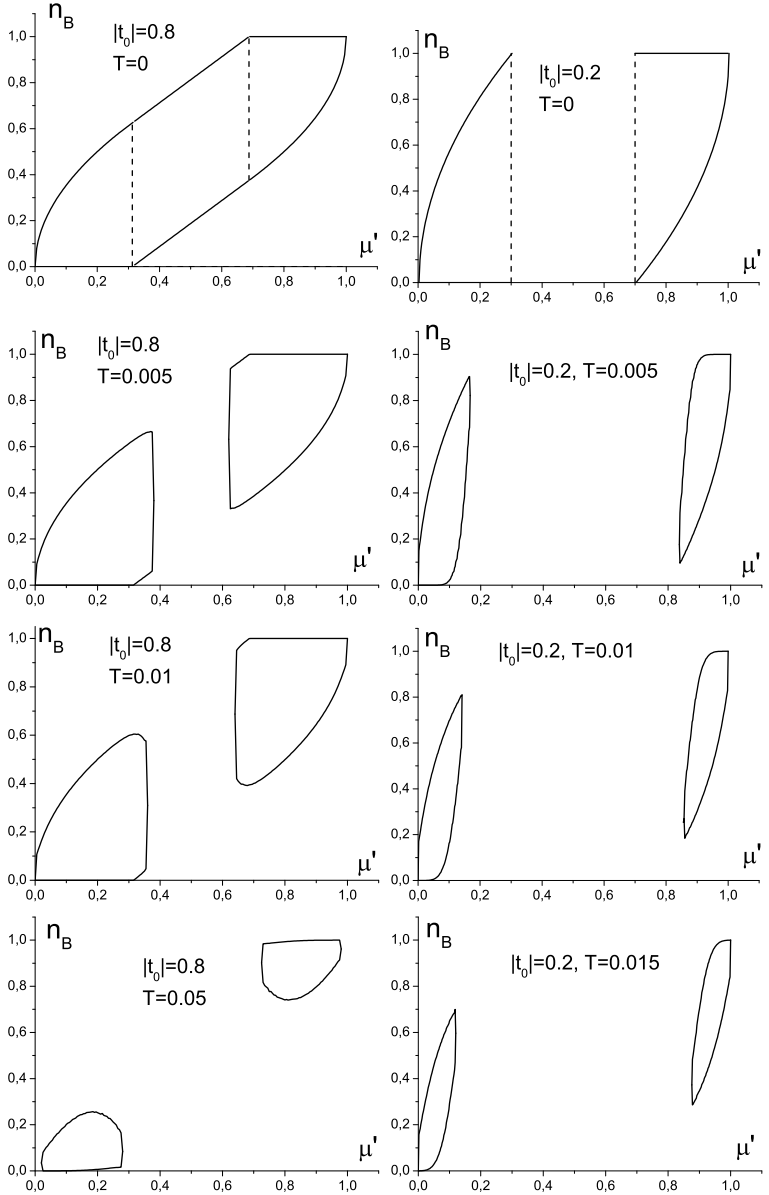

Figure 15. $(\overline{n}_B, \mu')$ diagrams illustrating the values of boson concentration $\overline{n}_B$ on the lines of the 1st order PT.

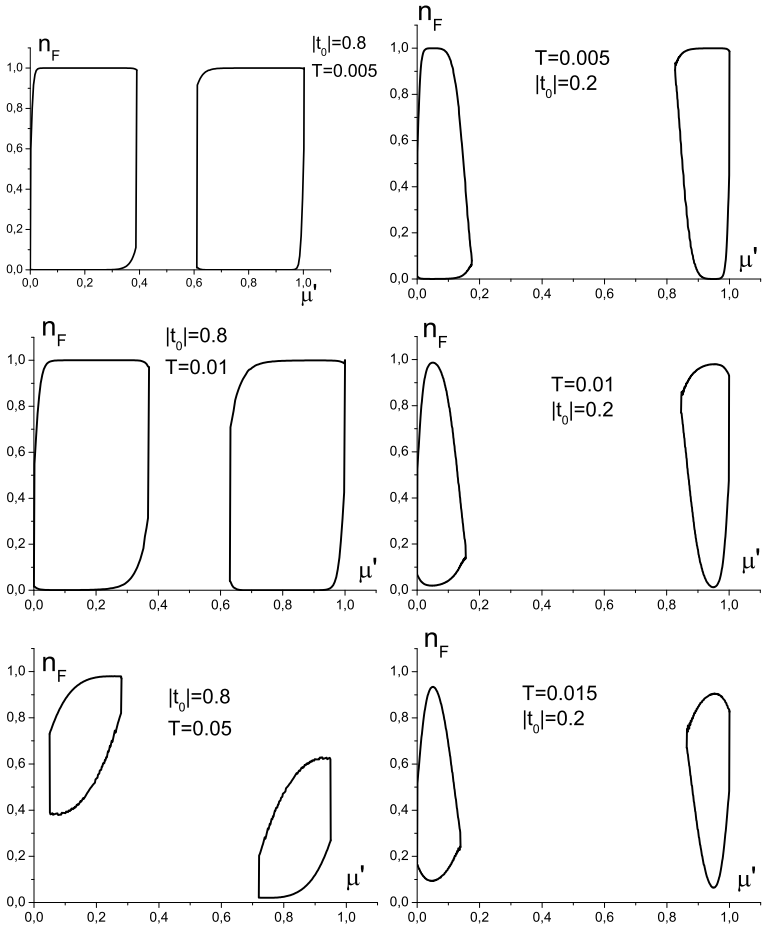

Figure 16. $(\overline{n}_F, \mu')$ diagrams illustrating the values of fermion concentration $\overline{n}_F$ on the lines of the 1st order PT.

intermediate concentration of bosons exists on the background of high fermion concentration. In this situation the phase segregation effect is a consequence of an on-site repulsion ($U' > 0$) between bosons and fermions.

5. Conclusions

We have considered in this work the thermodynamics of the mixture of the Bose- and Fermi-atoms in optical lattice basing on the Bose-Fermi-Hubbard model and restricting ourselves to the case of "heavy" fermions (that corresponds to the $t_F \to 0$ limit) as well as the repulsive on-site boson-fermion interaction ($U' > 0$). The approach of spinless fermions and hard-core bosons is used; the initial model reduces in this case to the four-state one. Our aim was to study the conditions, at which the MI-SF phase transition in such a model occurs. In the procedure we have employed, the U' interaction is taken exactly into account (using the formalism of Hubbard operators acting on the single-site basis of states). The boson hopping between the lattice sites is considered within the mean field approximation.

Investigation was performed in the thermodynamical regime of fixed values of chemical potentials of bosons (μ) and fermions (μ'). Equilibrium values of the order parameter $\varphi = \langle b \rangle = \langle b^+ \rangle$ (related to the BE condensate) were found from the global minimum condition of grand canonical potential Ω. Starting from equation for φ, we have considered the conditions of instability (at $T \neq 0$) of the normal (MI) phase with respect to condensation of bosons. As a results, the spinodal curves were calculated. Outside the $[0, U']$ interval for μ', the curves of spinodals have the usual dome-like shape. Attaining to this area, the curves undergo an appreciable deformation, and when they enter inside, the regions with two temperatures of instability, corresponding to one value of μ, appear. With the change of T the "re-entrant" transitions became possible. To get the real (T, μ) phase diagrams, we investigated the grand canonical potential behaviour in such regions.

The conditions were found at which the PT lines do not coincide with spinodals and the transitions become of the 1st order (instead of the 2nd one). The corresponding phase diagrams (T, μ) were built. Two different cases realize here. In the first one the 1st order PT line delimits the regions of MI and SF phases; the region of existence of SF phase is wider than limited one by spinodals. Such a line terminates at certain temperature in the tricritical point, transforming into the line of the 2nd order PT. In the second case the 1st order PT line is placed entirely

within the SF phase region and terminates at raising of temperature in the standard critical point (with coordinates μ_c, T_c). At $T = 0$, it divides this region into parts with BE condensate of different type: $\mathrm{SF}^{(\tilde{1}')}$ region, where all fermion states are filled, and $\mathrm{SF}^{(1')}$ region, where fermions are absent [43]. The difference between these two types of BE condensate disappears gradually in case of nonzero temperatures. When $T > T_c$, there exists the only one BE condensate with intermediate fermion concentration, that varies continuously as function of μ.

The described above features of (T, μ) phase diagrams manifest themselves as contraction and further vanishing (at the increase of T) of the 1st order PT lines in the phase diagrams, built on the (μ', μ) plane. At temperatures above the tricritical ones only the 2nd order PT lines (the spinodals) remain. The SF regions, which are disconnected at $|t_0| < U'/2$, gradually narrow and more off one from another, disappearing finally at $T = T_c^0$. In the case $U'/2 < |t_0| < U'$, there exists only one SF region at low temperatures, but during raising of T the change of topology of phase diagram (μ', μ) occurs. The SF phase region becomes biconnected and such a splitting into two parts is realized at point with coordinates $\mu = \mu' = 0,5U'$. For these values of chemical potentials we have at $\Theta = \Theta_c$ the second order phase transition from the SF to MI phase. Similarly to the previous case, at the further increase of temperature the separate SF regions become narrower and disappear at the same temperature T_c^0.

We have also investigated the symmetric case $\mu = U'/2$ (which corresponds to the boson half-filling ($\overline{n}_B = 1/2$). Consideration of thermodynamics of the model greatly simplifies here. The order parameter φ and critical temperature Θ_c do not depend on chemical potential of fermions μ' in this case. The fermion subsystem has an effect on temperature of transition to the state with BE condensate only through interaction U' with bosons. Here, the critical value $U'_{crit} = 2|t_0|$ exists. When U' exceeds such a value, SF phase in symmetrical case $\mu = U'/2$ disappears.

An additional insight into the physics of considered phase transitions in the boson-fermion mixture give the ($|t_0|$, μ) phase diagrams. Contrary to the standard hard-core boson model, where the diagrams of such a type are reflection-symmetric with respect to the point $\mu = 0$, in our case this symmetry is broken. Due to interaction of bosons with fermions, the ($|t_0|$, μ) diagrams are now symmetric with respect to transformation $\mu \to U' - \mu$, $\mu' \to U' - \mu'$. SF phase can exist when hopping parameter $|t_0|$ exceeds the minimum value $|t_0|_{min}$. The latter is determined by position of chemical potential of fermions μ' and increases at the temperature growth. Along with that, the SF region widens at

the beginning, but becomes narrower after that and disappears at high enough temperatures. Such an effect for mixtures with "heavy" fermions has been mentioned in [36] in the case of half filling.

The jumps of concentration $\bar{n}_B$ at crossing of the 1st order PT line during transition between MI and SF phases are an indication of possibility of the phase separation in the system (when one could fix the intermediate value of boson concentration). Segregation on SF and MI regions will take place in such a situation.

Direct comparison of calculated phase diagrams with the available data for the BFH model, concerning the equilibrium states and phase transitions, and obtained in the another thermodynamical regime (of fixed fermion concentration $\bar{n}_f$ besides the given chemical potential μ of bosons), is a special task. Some discussion of this problem and the examples of cases, where such a comparison was possible, were given in [43] for $T = 0$ limit.

It should be stressed, at the same time, that application of the μ =const and μ' =const regime enabled to describe the effect of fermions on the transition to the SF phase in a mixed system (consisting of hard-core bosons and "heavy" fermions) and show that such a PT becomes of the 1st order in the some regions of chemical potential values and at low temperatures. The BE condensation is influenced in this case by competition between states with the high and low fermion occupancy.

References

1. Greiner M., Mandel O., Esslinger T., Hänsch T.H., Bloch I., Nature (London), 2002, **415**, 39.
2. Greiner M., Regal C.A., Jin D.S., Nature (London), 2003, **426**, 537.
3. Fisher M.P.A., Weichman P.B., Grinstein G., Fisher D.S.O., Phys. Rev. B, 1989, **40**, 546.
4. Jaksch D., Bruder C., Cirac J.I., Gardiner C.W., Zoller P., Phys. Rev. Lett., **1998**, 81, 3108.
5. Albus A., Illuminati F., Eisert J., Phys. Rev. A, 2003, **68**, 023606.
6. Elstner N, Monien H., Phys. Rev. B, 1999, **59**, 012184.
7. G.G. Batrouni G.G., R.T. Scalettar R.T., G.T. Zimanyi G.T., Phys. Rev. Lett., 1990, **65**, 1765.
8. Dirkerscheid D.B.M., van Oosten D., Denteneer P.J.H., Stoof H.T.C., Phys. Rev. A, 2006, **68**, 043623.
9. Sengupta K., Dupuis N., Phys.Rev. A, 2005, **71**, 033629.
10. Ohashi Y., Kitaura M., Matsumoto H., Phys. Rev. A, 2006, **73**, 033617.

11. Konabe S., Nikuni T., Nakamura M., Phys. Rev. A, 2006, **73**, 033621.
12. Stasyuk I.V., Mysakovych T.S., Condens Matter Phys., 2009, **12**, 539.
13. Bloch I., Nature Phys., 2005, **1**, 23.
14. Bloch I., Dalibard J., Zwerger W., Rev. Mod. Phys., 2008, **80**, 885.
15. Ultracold atoms in optical lattices: Simulating quantum many-body systems, Lewensteine M., Sanpera A., Ahufinger V., Oxford University Press, 2012.
16. van Otterlo A., Wagenblast K.-H., Baltin R., Bruder C., Fazio R., Schön G., Phys. Rev. B, 1995, **52**, 16176.
17. Yamamoto K., Todo S., Miyashita S., Phys. Rev. B, 2009, **79**, 094503.
18. Isacsson A., Girvin S.M., Phys. Rev. A, 2005, **72**, 053604.
19. Kimura T., Tsuchiya S., Kurihara S., Phys. Rev. Lett., 2005, **94**, 110403.
20. Pai R.V., Sheshadri K., Pandit R., Phys. Rev. B, 2008, **77**, 014503.
21. Best T., Will S., Schneider U., Hackenmüller L., van Oosten D., Bloch I., Lühmann D.-S., Phys. Rev. Lett., 2009, **102**, 030408.
22. Gunter K., Stoferle T., Moritz H., Kohl M., Essling T., Phys. Rev. Lett., 2006, **96**, 180402.
23. Ospelkans C., Ospelkans S., Humbert L., Ernst P., Sengst K., Bongs K., Phys. Rev. Lett., 2006, **97**, 120402.
24. Lühmann D.-S., Bongs K., Sengstock K., Pfannkuche D., Phys. Rev. Lett., 2008, **101**, 050402.
25. Tewari S., Lutchyn R.M., Das Sarma S., Phys. Rev. B, 2009, **80**, 054511.
26. Mering A., Fleischhauer M., Phys. Rev. A, 2008, **77**, 023601.
27. Jürgensen O., Sengstock K., Lühmann D.-S, Phys. Rev. A, 2012, **86**, 043623.
28. Fehrmann H., Baranov M., Lewenstein M., Santos L., Optics. Express, 2004, **12**, 55.
29. Cramer M., Eisert J., Illuminati F., Phys. Rev. Lett., 2004, **93**, 190405.
30. Feshbach H., Ann. Phys., 1958, **5**, 337.
31. Inouye S., Andrews M.R., Stenger J., Miesner H.-J., Stamper-Kurn D.M., Ketterle W., Nature, 1998, **392**, 151.
32. Fehrmann H, Baranov M.A., Damski B., Lewenstein M., Santov L., Optics Communications, 2004, **243**.
33. Lewenstein M., Santos L., Baranov M.A., Fehrmann H., Phys. Rev. Lett.,2004, **92**, 050401.
34. Büchler H.P., Blatter G., Phys. Rev. Lett., 2003, **91**, 130404.

35. Polak T.P., Kopeć T.K., Phys. Rev. A, 2010, **81**, 043612.
36. Refael G., Demler E., Phys. Rev. B, 2008, **77**, 144511.
37. Titvinidze I., Snoeck M., Hofstetter W., Phys. Rev. Lett., 2008, **100**, 100401.
38. Bijlsma M.J., Herings B.A., Stoof H.T.C., Phys. Rev. A, 2000, **61**, 053601.
39. Heiselberg H., Pethick C.J., Smith H., Viverit L., Phys. Rev. Lett., 2000, **85**, 2418.
40. Viverit L., Giorgini B., Phys. Rev. A, 2002, **66**, 063604.
41. Bukov M., Pollet L., Phys. Rev. B, 2014, **89**, 094502.
42. Mathey L., Wang D.W., Hofstetter W., Lukin M.D, Delmer E., Phys. Rev. Lett., 2004, **93**, 120404.
43. Stasyuk I.V., Krasnov V.O., Condens. Matter Phys., 2015, **18**, 43702.
44. Mahan G.D., Phys. Rev. B, 1976, **14**, 780.
45. Micnas R., Ranninger J., and Robaszkiewicz S., Rev. Mod. Phys., 1990, **62**, 113.
46. Sengupta K., Dupuis N., Majumdur P., Phys. Rev. A, 2007, **75**, 063625.
47. Stasyuk I.V., Velychko O.V., Condens. Matter Phys., 2011, **14**, 13004.
48. Stasyuk I.V., Vorobyov O., Condens. Matter Phys., 2013, **16**, 23005.
49. Krasnov V.O., Ukr. J. Phys., 2015, **60**, 443.

CONDENSED MATTER PHYSICS

The journal **Condensed Matter Physics** is founded in 1993 and published by Institute for Condensed Matter Physics of the National Academy of Sciences of Ukraine.

AIMS AND SCOPE: The journal **Condensed Matter Physics** contains research and review articles in the field of statistical mechanics and condensed matter theory. The main attention is paid to physics of solid, liquid and amorphous systems, phase equilibria and phase transitions, thermal, structural, electric, magnetic and optical properties of condensed matter. Condensed Matter Physics is published quarterly.

ABSTRACTED/INDEXED IN: Chemical Abstract Service, Current Contents/Physical, Chemical&Earth Sciences; ISI Science Citation Index-Expanded, ISI Alerting Services; INSPEC; "Referatyvnyj Zhurnal"; "Dzherelo".

CONTACT INFORMATION:
Institute for Condensed Matter Physics
of the National Academy of Sciences of Ukraine
1 Svientsitskii Str., 79011 Lviv, Ukraine
Tel: +38(032)2761978; Fax: +38(032)2761158
E-mail: cmp@icmp.lviv.ua http://www.icmp.lviv.ua